Advanced Energy Conversion. Vol. 3, pp. 455–479. Pergamon Press, 1963. Printed in Great Britain

# SERIES RESISTANCE EFFECTS ON SOLAR CELL MEASUREMENTS*

MARTIN WOLF and HANS RAUSCHENBACH†

**Abstract**—Current–voltage characteristics of photovoltaic solar energy converter cells are obtainable by three methods, which yield different results due to the effects of the cell internal series resistance. The three resultant characteristics are: (1) the photovoltaic output characteristic, (2) the *p–n* junction characteristic, and (3) the rectifier forward characteristic. Choice of the proper method is necessary for obtaining the correct information for the individual application.

Most frequently used, e.g. for the determination of solar converter performance, is the photovoltaic output characteristic. A quick way is described for deriving such a characteristic for any light level from a corresponding characteristic obtained at a different light level. This method involves two translations of the coordinate system and requires only the knowledge of the series resistance and the difference in light intensities or short circuit currents.

An inversion of this method permits an easy determination of the series resistance, involving measurements at two arbitrary light levels of unknown magnitude.

The effects of series resistance consist at high light levels in a flattening of the photovoltaic output characteristic and a related drop in the maximum power point voltage. The resultant decrease in efficiency has to be overcome by series resistance reduction for solar cell applications with optical concentrators or for space missions in closer sun-proximity. In cell portions progressively further distant from the contact strip increasing cell voltages develop, approaching open circuit condition at very high light intensities. This yields a reduction of current contribution from those portions of the cell and a deviation from the normal proportionality between short circuit current and light intensity.

The direct measurability of the *p–n* junction characteristic at high current densities without series resistance effects by the second method provides a powerful tool to the device development engineer, besides yielding a second method for the determination of the series resistance. Results from the application of this method indicate that, in the current density range as used in solar energy conversion, the silicon solar cell characteristic is much more closely described by the diffusion theory for *p–n* junctions than was previously believed.

## 1. INTRODUCTION

LIKE all other known generators of electrical power, solar cells possess some internal series resistance. This internal series resistance is so important as to determine the current–voltage characteristic of most of these power generators. This is, however, not the case with the solar cells. Rather a *p–n* junction, internally contained in the solar cell, determines the current–voltage characteristic of the device, with the series resistance contributing only in a secondary manner. Nevertheless, the internal series resistance is of sufficient importance to have caught the attention of the device development engineers, which led to its reduction through decrease of contact resistance and through application of grid-shaped contacts. Also the power systems engineer concerned with the application of solar cells has to pay attention to the cell series resistance for the proper evaluation of current–voltage characteristics, for the matching of cells and for the prediction of solar cell output at differing light intensities. In order to further spread the knowledge about the various effects of the internal series resistance and about their proper interpretation, a summary of the series resistance effects on solar cell measurements and applications is presented in the following paragraphs.

* This paper was presented at the 1961 Pacific General Meeting of the AIEE, Salt Lake City, Utah, August 23–25, 1961.

† Heliotek, Division of Textron Electronics, Inc., 12500 Gladstone Avenue, Sylmar, California, U.S.A.

## 2. THE THREE CURRENT–VOLTAGE CHARACTERISTICS OF SOLAR CELLS

Current–voltage characteristics for solar cells can and have in the past been obtained by three different methods.

The most commonly used method applies a fixed illumination, usually of known intensity, and a resistive load which is varied between short circuit and open circuit conditions, while measuring the voltage across the solar cell terminals and the current out of these terminals [1]. This method of measurement applies to the solar cell in its normal photovoltaic mode of operation, and the current–voltage characteristic obtained in this manner is therefore called the "photovoltaic output characteristic." Figure 1(a) top shows the circuit diagram for this type of measurement, including the generally applied equivalent circuit diagram for the solar cell [2–4]. Since this paper is primarily concerned with measurements for applications of photovoltaic cells at relatively high current densities, effects of shunt resistance can be neglected and are therefore not even mentioned in most cases discussed. The following equation is frequently used to describe the current–voltage characteristic obtained by this method:

$$I = I_0 \left\{ \exp \left[ \frac{q}{AkT} (V - IR_s) \right] - 1 \right\} - I_L \tag{1}$$

This equation reproduces the obtained characteristics sufficiently well for most cases. Since a solar cell acts as a generator in this test, the current–voltage characteristic is obtained in the fourth quadrant of the current–voltage plane. The quantity $I_L$, called the light generated current, is proportional to the incident light intensity, if the spectral distribution of the radiation is not varied. The magnitude of this current is further determined by material and geometry factors of the solar cell, but is independent of the current–voltage characteristics. Other quantities of equation (1) are the terminal current and voltage, $I$ and $V$ respectively, and the internal series resistance $R_s$; $I_0$ is the diode saturation current determined by material properties; $q$ and $k$ are the electronic charge and the Boltzmann constant, respectively, while $T$ is the absolute temperature and $A$ a dimensionless constant between 1 and 5, but in most solar cells near 2·5 to 3.

The second method tests the solar cell like a diode without application of any illumination, but by supplying d.c. power from an external bias supply (see Fig. 1(a) center). The current–voltage characteristic obtained in this manner is therefore called the "diode forward characteristic". Again the voltage across the solar cell terminals and the current into these terminals are measured. The characteristic obtained by this method falls into the first quadrant of the current–voltage plane. It is described by:

$$I = I_0 \left\{ \exp \left[ \frac{q}{AkT} (V - IR_s) \right] - 1 \right\} \tag{2}$$

The diode forward characteristic differs from the photovoltaic output characteristic described by equation (1) by the absence of the light generated current $I_L$ and by the resulting positive direction of the terminal current $I$.

The third method for obtaining current–voltage characteristics from a solar cell appears more sophisticated than the previous two. The solar cell is again illuminated, but in this case with variable light intensity. The amount of the illumination does not have to be known, if the value of the light generated current $I_L$ can be determined. This condition is fulfilled when the magnitude of the cell series resistance is sufficiently small so that the output current $I$ of the device, when measured by the photovoltaic output method, is

constant for all terminal voltages between 0 and 0·1 volts. In this case the measuring circuit may consist of a switch, a high resistance voltmeter and a low resistance milliamperemeter, arranged as shown in the cirtuit diagram (Fig. 1(a) bottom). The voltage drop across the milliamperemeter should be less than 50 mV and the resistance in the voltmeter circuit

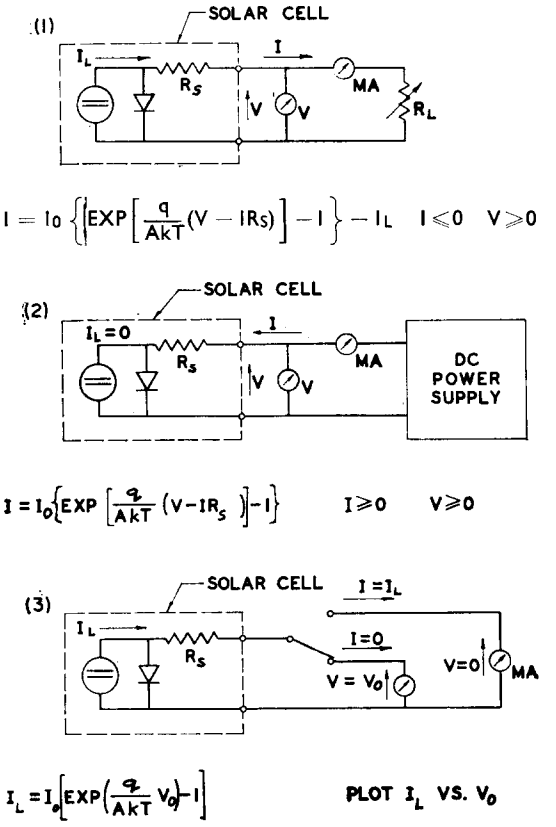


FIG. 1(a). Three methods for obtaining current-voltage characteristics on solar cells.
(1) Photovoltaic output (constant illumination).
(2) Diode forward (without illumination).
(3) *P–N* junction (variable illumination).

more than 100 k$\Omega$. The measurement consists of determining the short circuit current, $I_{sc}$, which under the presented conditions equals the light generated current $I_L$, and the open circuit voltage $V_0$ for every light intensity setting. Each pair of corresponding short circuit current and open circuit voltage values is plotted as one point in the first quadrant of the current–voltage plane. Through the variation of the light intensity, a succession of such points is obtained which presents the desired current–voltage characteristic. A method very similar to the one described here was first applied by Heeger and Nisbet for the matching of solar cells [5], and was again used independently from the investigations described

later in this paper for similar studies by Queisser [6]. If at higher light intensities the condition of flatness of the photovoltaic output characteristic near zero voltage is not fulfilled, then the light intensity will have to be measured independently, its value expressed in

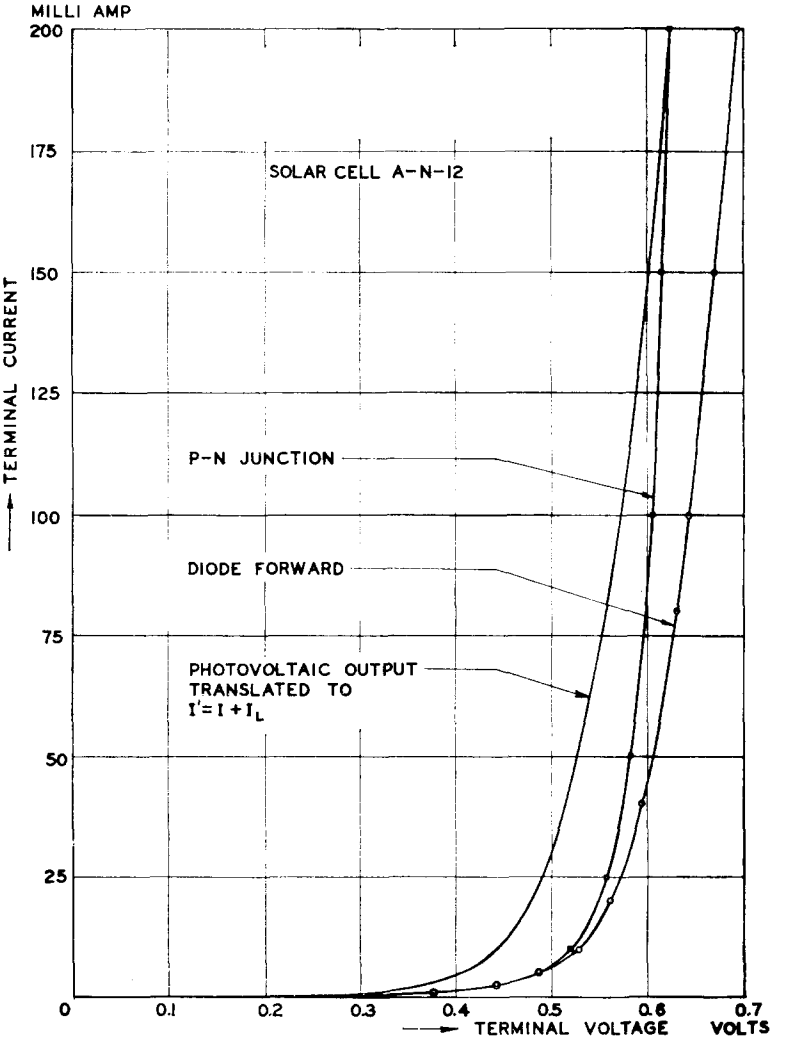


FIG. 1(b). Three current-voltage characteristics obtainable on the same solar cell.

equivalent light generated current, and in this form entered into the graph. The measurement of light intensity can be performed by means of a more suitable solar cell, or of other photometric devices. The current–voltage characteristic obtained by this method is described by equation (3):

$$I_L = I_0 \left[ \exp \frac{q}{AkT} V_0 - 1 \right] \tag{3}$$

It is derived from equation (1) for the photovoltaic output characteristic by setting $I = 0$ and replacing $V$ by the open circuit voltage $V_0$. In this case the term containing the internal series resistance $R_s$ vanishes. The resultant expression is identical to that for the diode forward characteristic except for the absence of the series resistance term.

Figure 1(b) shows the current–voltage characteristics obtained on the same solar cell by applying the three methods described. A translation $I' = I + I_L$ has, however, been applied to the photovoltaic output characteristic in order to move it into the first quadrant of the current–voltage plane and to make it pass through the origin of this plane, thus facilitating comparison with the other two characteristics. The observed differences between the three characteristics are readily understandable from the previous description of the three methods for their generation. In the photovoltaic output characteristic, a current is generated internally in the cell, giving rise to a voltage across the $p$–$n$ junction in the forward bias direction and causing current flow through this $p$–$n$ junction. The difference in current between the light generated current $I_L$ and the forward current through the $p$–$n$ junction flows through the device terminals, but also results in a voltage drop across the internal series resistance. The measured terminal voltage is therefore smaller than the voltage across the $p$–$n$ junction by the amount of this voltage drop. In the diode forward characteristic, the current is supplied from an external power supply, not using the internal generator. All of the current passing the solar cell terminals flows through the $p$–$n$ junction, but it passes the internal series resistance in the opposite direction than it does in the case of the photovoltaic output characteristic. Therefore the voltage across the $p$–$n$ junction is smaller than the terminal voltage $V$. In the $p$–$n$ junction characteristic finally a case is obtained in which the effect of the internal series resistance is eliminated. In the open circuit voltage condition, the terminal voltage is identical to the voltage existing across the $p$–$n$ junction, while the short circuit current measures the light generated current directly as long as the voltage drop across the internal series resistance is sufficiently small as to cause only a negligibly small current to flow through the $p$–$n$ junction in the forward direction.

The curves of Fig. 1(b) substantiate this explanation. The photovoltaic output characteristic exhibits terminal voltages which are smaller than those of the $p$–$n$ junction characteristic by the voltage drop over the internal series resistance caused by the current flowing through this part of the circuit. Conversely, the diode forward characteristic exhibits voltage values higher than those of the $p$–$n$ junction characteristic by the voltage drop caused by the current flow through the internal series resistance.

The foregoing discussions also outline the range of application for the different types of characteristics. Whenever the performance of a solar cell as a photovoltaic energy converter is concerned, be it for the determination of its power output, for the matching of different solar cells into a system, or for the extrapolation of the cell output from one intensity level to a different one, then one has to use the photovoltaic output characteristic. If the characteristic of the $p$–$n$ junction itself is to be studied, then the $p$–$n$ junction characteristic obviously has to be obtained. If the solar cell is to be used as a passive device and its performance without illumination is to be studied, then the diode forward characteristic has to be taken.

## 3. THE EFFECT OF SERIES RESISTANCE ON THE RELATIONSHIP BETWEEN SHORT-CIRCUIT CURRENT AND LIGHT INTENSITY

The light generated current $I_L$ is proportional to the intensity of the incident radiation up to extremely high light intensities. Numerous measurements undertaken in order to

check this relationship appeared to show deviations at light intensities orders of magnitude below those where deviations can be expected. These supposed deviations were caused by the effect of the series resistance on the short circuit current which had been measured instead of the light generated current. Such a substitution can properly be made on ideal solar cells with zero series resistance, and on real solar cells at sufficiently low light intensities only. At light intensities high enough so that the product of internal series resistance and terminal current exceeds 250 mV, the short circuit current can no longer be considered identical to the light generated current.

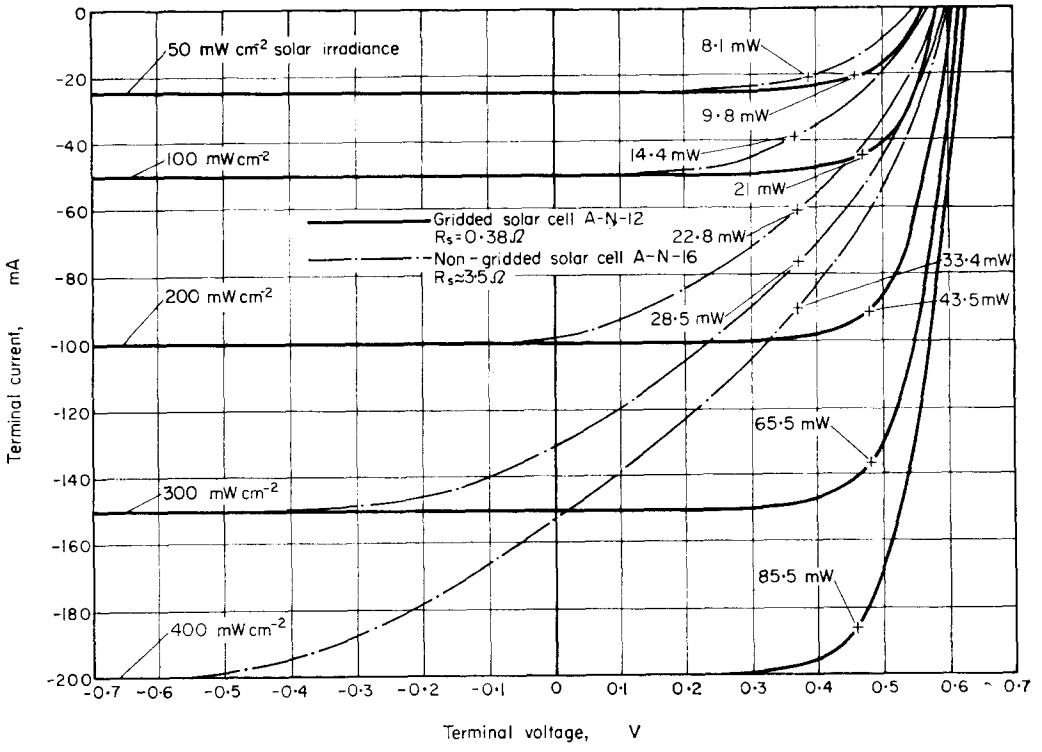


FIG. 2.

Figure 2 illustrates this fact on the photovoltaic output characteristics of two different solar cells taken at five values of solar irradiance between 50 mW cm$^{-2}$ and 400 mW cm$^{-2}$. One of these solar cells is a gridded solar cell with a series resistance of 0·38 $\Omega$, while the other solar cell is a nongridded cell having a series resistance of about 3·5 $\Omega$. The low-series resistance cell exhibits rather square characteristics up to 400 mW cm$^{-2}$ of solar irradiance, with the terminal current staying constant for variations of the terminal voltage from 0 to 200 mV. This means that the short circuit current is identical to the light generated current throughout this irradiance range. The high-series resistance cell, however, exhibits successively more rounded characteristics at increasing light intensities, and the short circuit current deviates from the light generated current already at 200 mW cm$^{-2}$ of solar irradiance. At larger values of solar irradiance, the terminal current does not reach its maximum value at zero terminal voltage, but continues to increase with increasing negative terminal voltages, until it finally reaches its maximum value and equals the light generated

current. The photovoltaic output characteristic can readily be extended into the third quadrant of the current–voltage plane, if the resistive load is provided by an external source which permits the simultaneous application of negative voltages.

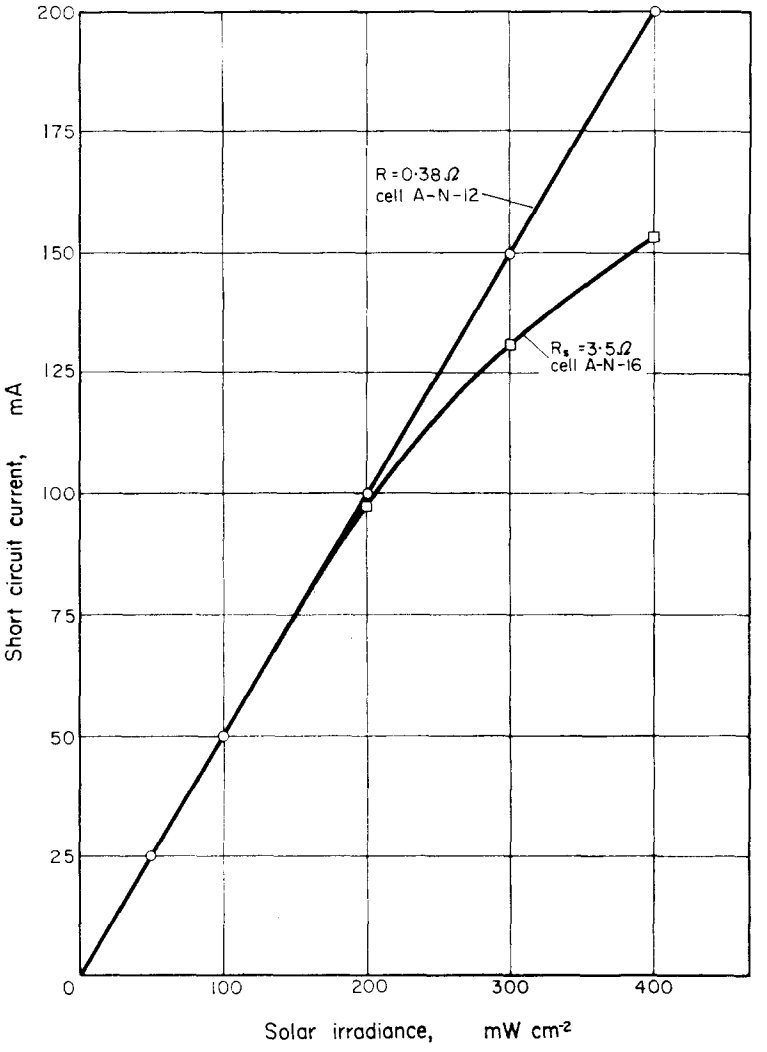


FIG. 3. Short circuit current versus solar irradiance at different internal series resistance values.

Figure 3 presents a plot of the short circuit current as a function of solar irradiance for the two cells used for the measurements presented in Fig. 2. This plot shows that the low series resistance cell exhibits a linear relationship between short circuit current and solar irradiance up to 400 mW $cm^{-2}$ which is identical to four times the maximum solar irradiance reached at the earth's surface at sea level at noon time on a clear day. The graph also shows the considerable deviation from linearity for the solar cell with the high internal series resistance.

The cause for the deviation of the short circuit current from the light generated current at high light intensity and with large series resistance, particularly with large diffused layer sheet resistance, lies in the voltage drop across this series resistance. This voltage drop can result in an appreciable voltage across the $p$–$n$ junction in portions of the cell, although zero voltage condition exists at the terminals.

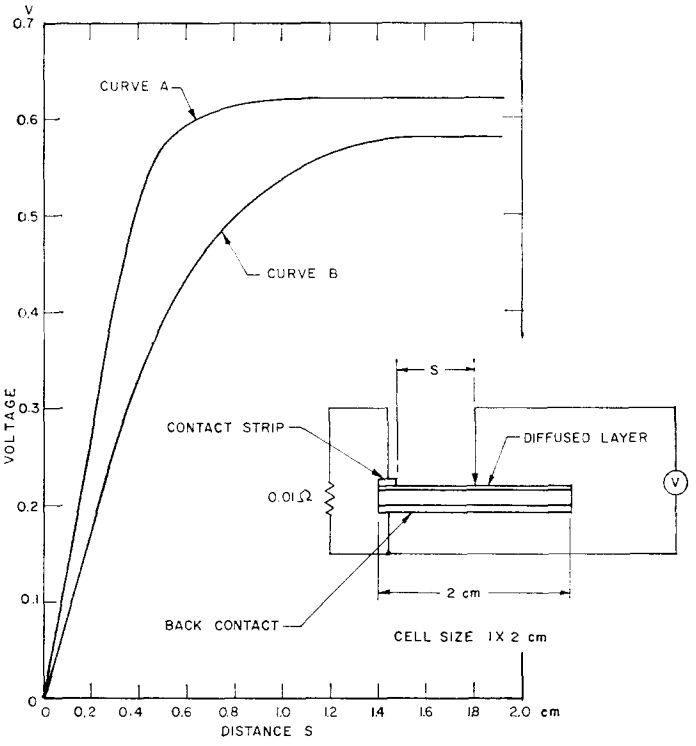


| | CURVE A | CURVE B |
|---|---|---|
| LIGHT INTENSITY | 400 mW/cm$^2$ | 200 mW/cm$^2$ |
| CELL OPEN CURRENT VOLTAGE | 0.620 V | 0.580 V |

FIG. 4. Diffused layer voltage versus distance from contact strip, cell terminals short circuited.

This effect is illustrated in Fig. 4. A fine tungsten wire probe which causes only a negligible shadow makes contact with the illuminated diffused layer. This probe is moved across this layer along a line perpendicular to the contact strip, while the contact strip itself is shorted to the back contact of the cell. The voltages, measured with a high-resistance voltmeter connected as shown in Fig. 4, are then plotted against the corresponding distances of the probe from the contact strip. Near the terminal strip, the voltage increases practically linearly with distance from the contact, then increases more slowly and finally, when the cell open circuit voltage is reached, remains constant. This saturation at large distances from the contact has two reasons: (a) the density of the current flowing in the diffused layer toward the contact strip decreases with distance from the contact, and (b) with in-

creasing voltages across portions of the cell the current contribution from those portions is reduced (compare with current–voltage curves such as Fig. 2).

Even if solar cells are operated at light intensities such that the current density in the diffused layer is lower than required for saturation, high enough voltages may develop in portions of the cell to cause a substantial reduction in the current contributed from the corresponding regions of the cell. This mechanism appears to be the only one by which the cell can maintain short circuit conditions at its terminals, thereby explaining the aforementioned differences between short circuit current and light generated current.

The foregoing discussion emphasizes the caution which has to be used in the application of the short circuit current of a solar cell for light metering purposes at high light intensities. The amount of internal series resistance in the cell has to be determined and the region of deviation from the linearity be established before a cell can be confidently applied for such purposes.

## 4. THE EFFECTS OF INTERNAL SERIES RESISTANCE ON SOLAR CELL PERFORMANCE

The curves of Fig. 2 indicate that the internal series resistance can severely affect the performance of photovoltaic cells as solar energy converters. The maximum power output of a solar cell is given by the area of the largest rectangle that can be drawn inside the photovoltaic output characteristic. The area of such a rectangle increases with increasing "sharpness" of the knee in the photovoltaic output characteristic. Internal series resistance causes a successively larger "rounding" of the characteristic at increasing light intensities. Solar cells are normally designed for best performance at radiation intensities as obtained at the earth's surface. Such cells may therefore not give optimum performance at increased light intensities as may be encountered in space vehicle applications in closer proximity to the sun or in the use of solar cells combined with radiation concentrating devices.

Figure 5 presents three sets of curves, calculated for a solar cell with $I_0 = 6{\cdot}9 \times 10^{-12}$ A, $I_L = 5{\cdot}5 \times 10^{-2}$ A, and $q/AkT = 38{\cdot}6\ \mathrm{V}^{-1}$, and with assumed internal series resistance values of 0, 0·5 and 1·0 $\Omega$. The curves give the maximum power output into a matched load, the maximum power point voltages and the efficiencies for values of solar irradiance between 50 and 350 mW/cm$^2$. The zero-resistance solar cell shows monotonously increasing power output with increasing light intensity. Finite values of the series resistance cause the maximum power output to increase less rapidly at the higher light intensities. This effect becomes progressively larger with increasing series resistance and light intensity.

The maximum power point voltage, which steadily increases with increasing light intensity for the zero-series resistance cell, starts to decrease at higher light intensities for the cell with 0·5 $\Omega$ series resistance, and shows continuous and larger decrease at a series resistance value of 1·0 $\Omega$ through the intensity range of 50 to 400 mW cm$^{-2}$. The maximum power point voltage which steadily increases with light intensity for the zero-series resistance cell starts to decrease at the higher light intensities for the cell with 0·5 $\Omega$ series resistance, and shows a continuous drop at a series resistance value of 1·0 $\Omega$.

The dotted curves in Fig. 5 present the conversion efficiency. The curve for the zero-series resistance cell shows a monotonous rise toward the higher solar irradiance values while the curves for the 0·5 and the 1·0 $\Omega$ cells exhibit progressive efficiency decreases toward the higher light intensities.

Also presented in Fig. 5 are experimental curves obtained on two solar cells with 0·38 and 3·5 $\Omega$ series resistance, respectively. It is interesting to note that the shape of the experi-

mental curve for the 0·38 Ω cell fits perfectly into the system of the theoretical curves although its absolute values are somewhat lower due to deviations of other device parameters from those assumed for the theoretical evaluation. The information presented in this paragraph leads to the conclusion that for high power output and high efficiency at

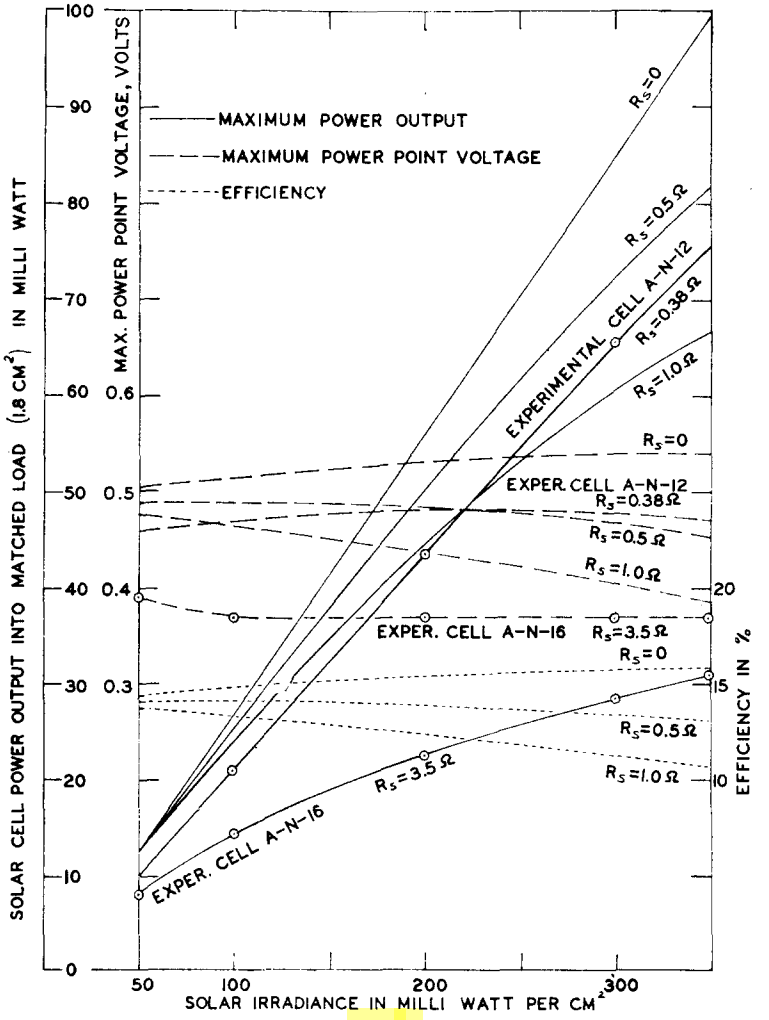


FIG. 5.

high light intensities, and for a minimum change of the maximum power point voltage with increasing light intensities, solar cells with progressively smaller internal series resistance will have to be selected or be specifically developed.

## 5. A METHOD FOR THE PREDICTION OF THE PHOTOVOLTAIC OUTPUT CHARACTERISTIC FOR DIFFERENT LIGHT LEVELS

The photovoltaic output characteristic as described by equation (1) permits an easy prediction of the corresponding current–voltage characteristic for a given light level which differs from the one at which the original characteristic has been measured.

In the case of the solar cell with zero-series resistance, the exponent of equation (1) contains only the independent variable, that is the terminal voltage. For any fixed light level only the exponential term is variable on the right-hand side of equation (1). Any change in the light intensity enters then into the relationship through the light generated current $I_L$. A change in the light intensity results, at constant terminal voltage $V$, in a change of the terminal current $I$ equal to the difference of the light generated currents $\Delta I_L$. This means that the shape of the curve, which is determined by the exponential term, is invariant with respect to light intensity. The mathematical derivation for this is presented in Appendix A of this paper. The photovoltaic output curve for a different value of light intensity can readily be obtained by translating the original curve parallel to the ordinate of the $IV$ coordinate system by an amount equal to the difference in the light generated currents, which is proportionate to the difference of the light intensities.

The method outlined in the previous paragraph is valid for solar cells with small values of series resistance or at sufficiently low light levels so that the effects of the series resistance can be neglected. This is expressed in the condition that the product $IR_s$ has to be negligibly small compared to the terminal voltage $V$. If this condition is not fulfilled, then a second translation parallel to the abscissa has to be performed on the photovoltaic output characteristic for the transformation to a second light intensity. The second translation consists in a decrease of the terminal voltage by an amount equal to the product of the internal series resistance $R_s$ and the difference in the light generated currents, $\Delta I_L$. A formal derivation for this case is also given in Appendix A.

For a change of the photovoltaic output characteristic from the light intensity $L_1$ with the light generated current $I_{L1}$ to the light intensity $L_2$ generating the current $I_{L2}$, the two translations

$$I_2 = I_1 - \Delta I_L \tag{4}$$

and

$$V_2 = V_1 - \Delta I_L R_s \tag{5}$$

have therefore to be performed. Since $I_L$ is proportional to the light intensity $I_L = CL$, $\Delta I_L$ can be expressed through a relationship between the light intensities:

$$\Delta I_L = C(L_2 - L_1) \tag{6}$$

Since $I_{L1}$ can be readily obtained from the photovoltaic output characteristic, measured at light intensity $L_1$, $\Delta I_L$ is more conveniently related to the difference in light intensities through the form:

$$\Delta I_L = I_{L1} \frac{L_1 - L_2}{L_1} \tag{7}$$

A previously expressed note of caution in the substitution of the short circuit current $I_{sc}$ for the light generated current $I_L$ at high light intensities or large value of series resistance should be observed.

Figure 6 illustrates the two translations of the coordinate system to be performed by going from a light intensity $L_1$ at which the photovoltaic output characteristic has been measured, to a higher light intensity $L_2$ at which this characteristic is desired to be known.

Figure 7 presents experimental data to demonstrate the correctness of this procedure. The photovoltaic output characteristics from Fig. 2 for the low series resistance solar cell, measured at five different light levels between 50 and 400 mW cm$^{-2}$, are reproduced in Fig. 7. After performing the translations of the coordinate system for the four photovoltaic

output curves obtained at the lower light intensities to the 400 mW cm$^{-2}$ level, they are found to all fall on top of each other as well as on the experimental curve for this intensity. The experimentally obtained curves are given in solid lines, while the transformed curves are presented by squares, circles, and triangles, corresponding to the different original intensities.

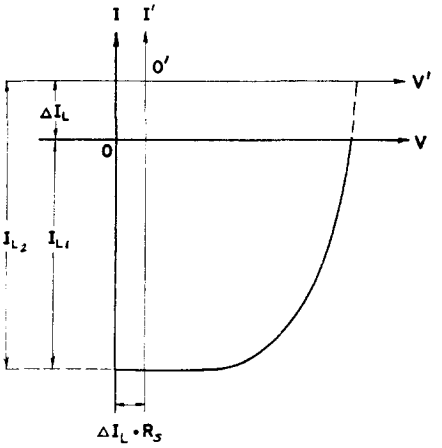


FIG. 6.

## 6. A METHOD FOR THE DETERMINATION OF THE INTERNAL SERIES RESISTANCE

An inversion of the method described in section 5 permits the easy and accurate determination of the internal series resistance of any solar cell. For this purpose the photovoltaic output characteristic has to be measured at two different light intensities, the magnitudes of which do not have to be known. The two characteristics are translated against each other by the amounts $\Delta I_L$ and $\Delta I_L \times R_s$ in the $y$- and the $x$-direction, respectively. Two corresponding points on the two characteristics show a displacement with respect to each other, which is identical to the two translations of the coordinate systems. The displacement parallel to the ordinate gives the value of $\Delta I_L$. Since the displacement parallel to the abscissa equals $\Delta I_L R_s$, the value of the internal resistance $R_s$ is readily obtained.

One practical approach to this procedure is to choose an arbitrary interval $\Delta I$ from the short circuit current $I_{sc}$, which determines the first characteristic. It is frequently found convenient to choose $\Delta I$ so as to obtain a point in or near the knee of the characteristic.The same $\Delta I$ value is used for the finding a second corresponding point on the second characteristic. An illustration of the procedure is presented in Fig. 8.

This method was first suggested in 1960 by Swanson [7].

## 7. EXPERIMENTALLY FOUND DEVIATIONS FROM THE LUMPED CONSTANT MODEL

It has been found that the measured current–voltage characteristics of many solar cells cannot be very accurately described by the equivalent circuit model of Fig. 1 and by equation (1). These deviations have been found to be due to two separate effects: one involving the $p$–$n$ junction characteristic, and the other the internal series resistance. The effect

involving the $p$–$n$ junction characteristic will be discussed in section 8, while in this section attention will be directed to the effect of the internal series resistance.

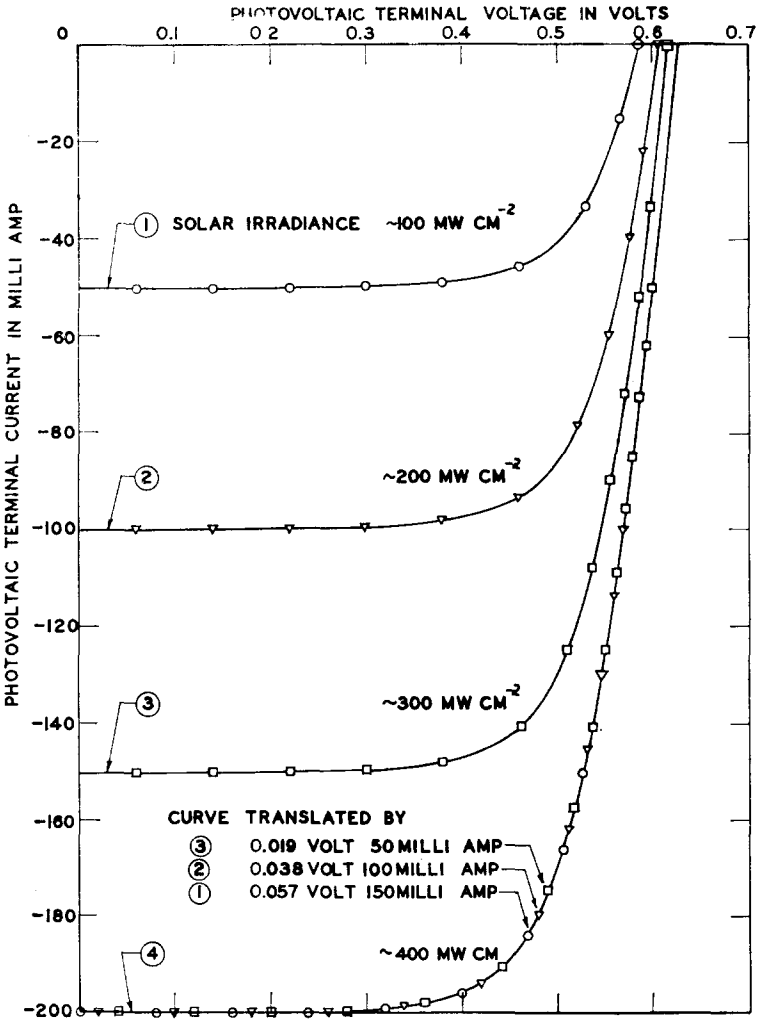


FIG. 7. Current–voltage characteristics of solar cell No. A–M–12 at different illumination levels.

If the model discussed in the previous sections is valid, then the same value of internal series resistance $R_s$ will be obtained by application of the method described in section 6, independent of the chosen value of $\Delta I$. Also, a sequence of photovoltaic output characteristics obtained at different light levels, and transformed to any one of these curves by the method described in section 5 will show perfect agreement between the individual curves as illustrated in Fig. 7. Equality of the series resistance values obtained from different parts of the characteristic, and agreement between transformed curves is, however, not found on all solar cells measured. The high series resistance cell A-N-16 used for obtaining

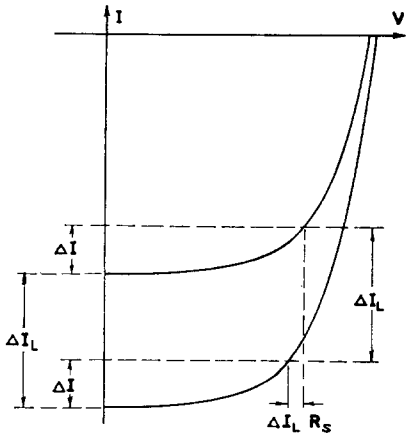
I
V
ΔI
ΔI_L
ΔI_L
ΔI
ΔI_L R_S

FIG. 8.

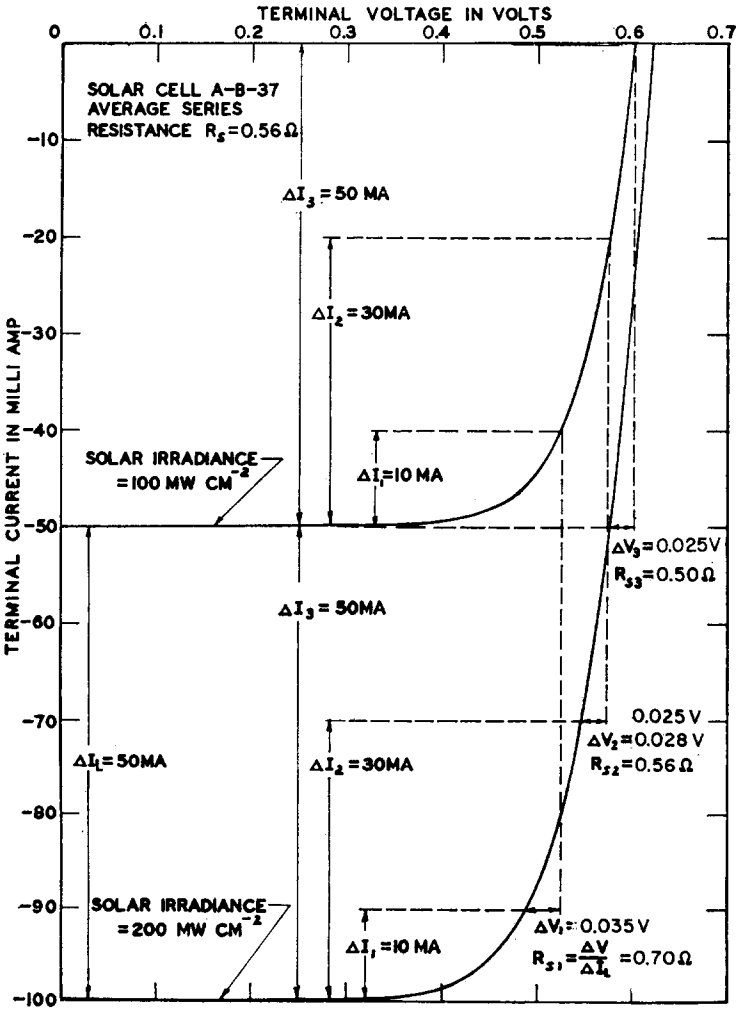
TERMINAL VOLTAGE IN VOLTS
0
0.1
0.2
0.3
0.4
0.5
0.6
0.7
SOLAR CELL A-8-37
AVERAGE SERIES
RESISTANCE R_S=0.56Ω
TERMINAL CURRENT IN MILLI AMP
-10
-20
-30
-40
-50
-60
-70
-80
-90
-100
ΔI_3=50 MA
ΔI_2=30MA
SOLAR IRRADIANCE
=100 MW CM^-2
ΔI_1=10 MA
ΔV_3=0.025V
R_S3=0.50Ω
ΔI_3=50MA
0.025 V
ΔV_2=0.028 V
R_S2=0.56Ω
ΔI_L=50MA
ΔI_2=30MA
SOLAR IRRADIANCE
=200 MW CM^-2
ΔI_1=10 MA
ΔV_1=0.035V
R_S1=ΔV/ΔI_L =0.70Ω

FIG. 9(a)

data for Figs. 2, 3 and 5 shows such deviations. These observations are not only made on cells with high internal series resistance, although the deviations found in low series resistance cells are generally substantially smaller.

VARIATION OF CURVE SHAPE WITH LIGHT INTENSITY OBSERVED ON CELL A-B-37

| CURVE NO. | SOLAR IRRADIANCE MW CM$^{-2}$ | SHIFT $\Delta I$ MA | SHIFT $\Delta I_L R_s$ MV |
|---|---|---|---|
| 1 | 50 | - | - |
| 2 | 100 | 25 | 13 |
| 3 | 200 | 75 | 39 |
| 4 | 300 | 125 | 63 |
| 5 | 400 | 175 | 90 |

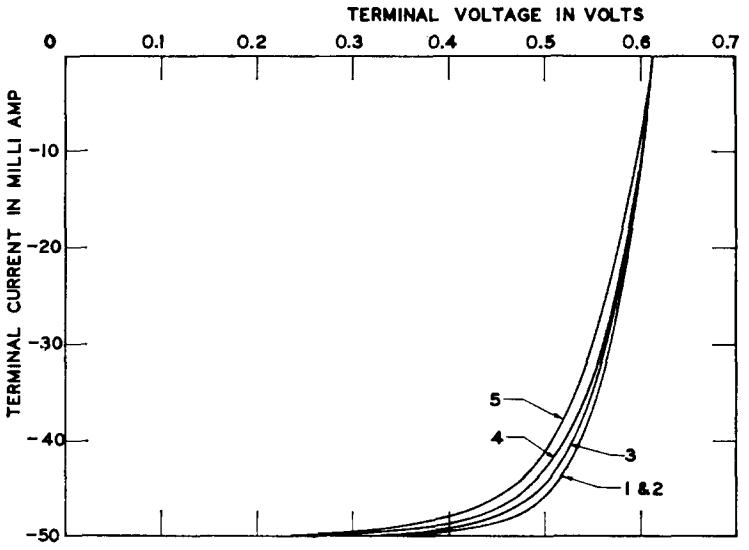


FIG. 9(b)

Figure 9(a) presents two curves obtained on a low series resistance gridded solar cell at two different light intensities. Marked in this figure are the series resistance values obtained at different portions of the characteristics. These values range from 0·5 to 0·7 $\Omega$. It has been observed, that the limits of the range of series resistance values are rather independent of the amount of light intensity and of the difference in light intensities used for this evaluation, except for the fact that at high light intensities a different portion of the curve can be evaluated which is not available at the low intensities. This is demonstrated by the data contained in Table 1, which were obtained on cell A-G-43.

TABLE 1. SERIES RESISTANCE VALUES OBTAINED ON SOLAR CELL A–G–43 AT DIFFERENT CORRELATION POINTS AND LIGHT INTENSITIES

| Initial solar irradiance ($mWcm^{-2}$) | Initial light generated current $\Delta I_{L1}$ (mA) | Final solar irradiance ($mWcm^{-2}$) | Final light generated current $I_{L2}$ (mA) | Light generated current difference $\Delta I_L$ (mA) | Correlation current difference $\Delta I$ (mA) | Measured series resistance $R_s$ ($\Omega$) |
|---|---|---|---|---|---|---|
| ~ 50 | 25·1 | ~100 | 50·1 | 25 | 2·7 | 0·4 |
| | | | | | 5·6 | 0·4 |
| | | | | | 12·1 | 0·4 |
| | | | | | 20·2 | 0·36 |
| | | | | | 25·1 | 0·36 |
| ~100 | 50·1 | ~200 | 100·0 | 49·9 | 10·0 | 0·36 |
| | | | | | 20·0 | 0·34 |
| | | | | | 30·0 | 0·36 |
| | | | | | 40·0 | 0·36 |
| | | | | | 49·9 | 0·32 |
| ~100 | 50·1 | ~300 | 150·0 | 100 | 5·0 | 0·58 |
| | | | | | 10·0 | 0·42 |
| | | | | | 25·0 | 0·37 |
| | | | | | 50·0 | 0·34 |
| ~100 | 50·1 | ~400 | 199 | 148·9 | 5·0 | 0·43 |
| | | | | | 25·0 | 0·37 |
| | | | | | 50·1 | 0·34 |
| ~100 | 50·1 | ~500 | 249·5 | 199·4 | 5·0 | 0·38 |
| | | | | | 25·0 | 0·39 |
| | | | | | 50·1 | 0·36 |
| ~300 | 150·0 | ~400 | 199 | 49 | 25 | 0·36 |
| | | | | | 150 | 0·30 |
| ~300 | 150·0 | ~500 | 249·5 | 99·5 | 25 | 0·42 |
| | | | | | 50 | 0·39 |
| | | | | | 75 | 0·37 |
| | | | | | 100 | 0·36 |
| | | | | | 125 | 0·34 |
| | | | | | 150 | 0·32 |

The reasons for the deviations are to be found in the physical configuration of the solar cell. Major contributions to the internal series resistance come from the sheet resistance of the *p*-layer, the bulk resistance of the *n*-layer, and the resistance between the semiconducting material and the metallic contacts. While the contact series resistance can properly be represented by a lumped resistance, the sheet resistance and the bulk resistance are distributed throughout the device. Figure 10 shows the transition from the physical configuration of the solar cell to the distributed constants model. The cell is imaginarily divided into many elements, each one containing a *p–n* junction, which acts as a source and a shunting diode simultaneously. These junction elements are inter-connected by the distributed resistances. This model was studied in 1958 by the first author as the proper representation for the current flow and voltage distribution in a solar cell, but has been discarded because of the enormous complexity of its evaluation. A similar, slightly simplified model has been proposed by Wysocki, Loferski and Rappaport in 1960 [8], but was apparently also not

evaluated. Because of the rather small values of internal series resistance encountered in the modern gridded solar cells, an intermediate model is proposed here. It represents the next refinement step from the lumped constants model of Fig. 1. Instead of dividing the cell into many elements, it splits the solar cell into two equal parts and adds the bulk re-

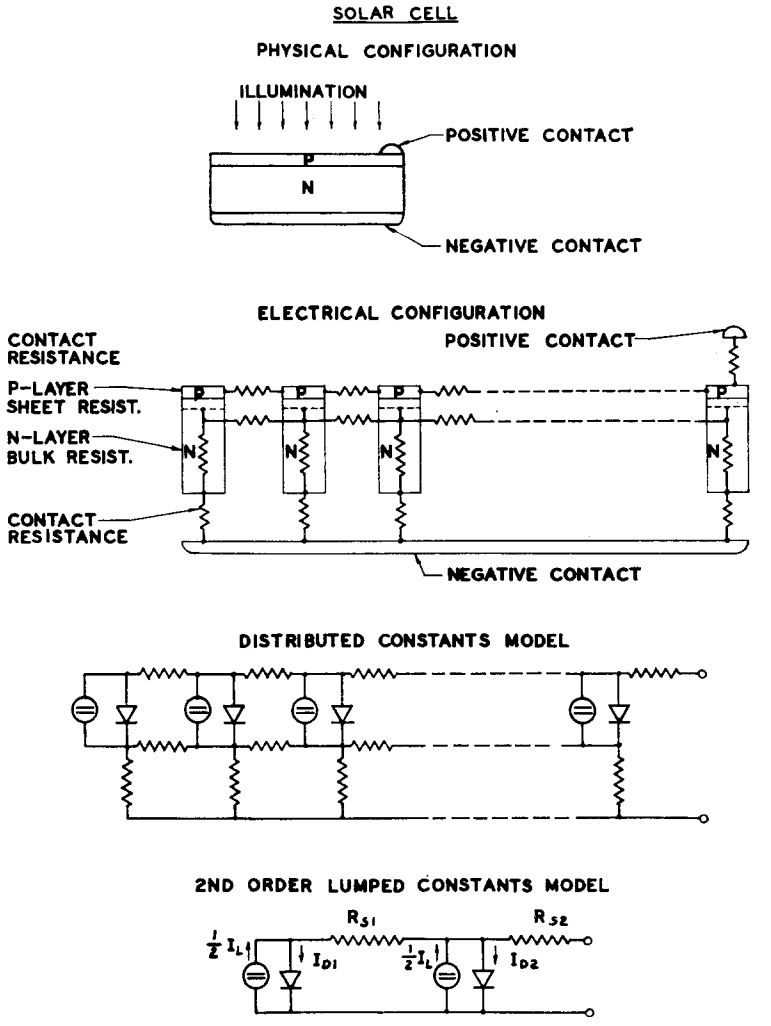


FIG. 10.

sistance, the contact resistance, and a portion of the sheet resistance into a lumped element next to the terminal. The other portion of the sheet resistance is placed in the connection between the two parts of the cell. The ratio between the values of the two resistance elements has been found to vary between individual cells.

Figure 12 presents the *p–n* junction characteristic of a silicon solar cell obtained by the third method described in section 2. It also presents theoretical points for the photovoltaic output characteristic derived from the *p–n* junction characteristic by using both the lumped constants model according to Fig. 1(a), and the improved lumped constants model of Fig. 10. Also presented is the experimentally obtained photovoltaic output characteristic

which demonstrates good agreement between the experimental data and the improved lumped constants model. A resistance ratio of 9 to 10 has been found to be appropriate for the cell evaluated for this figure.

## 8. APPLICATION OF THE *P–N* JUNCTION CHARACTERISTIC FOR DEVICE STUDIES

The diode forward characteristic has long been used for the investigation of device parameters like the saturation current, the constant $A$ in the exponent of the diode charac-

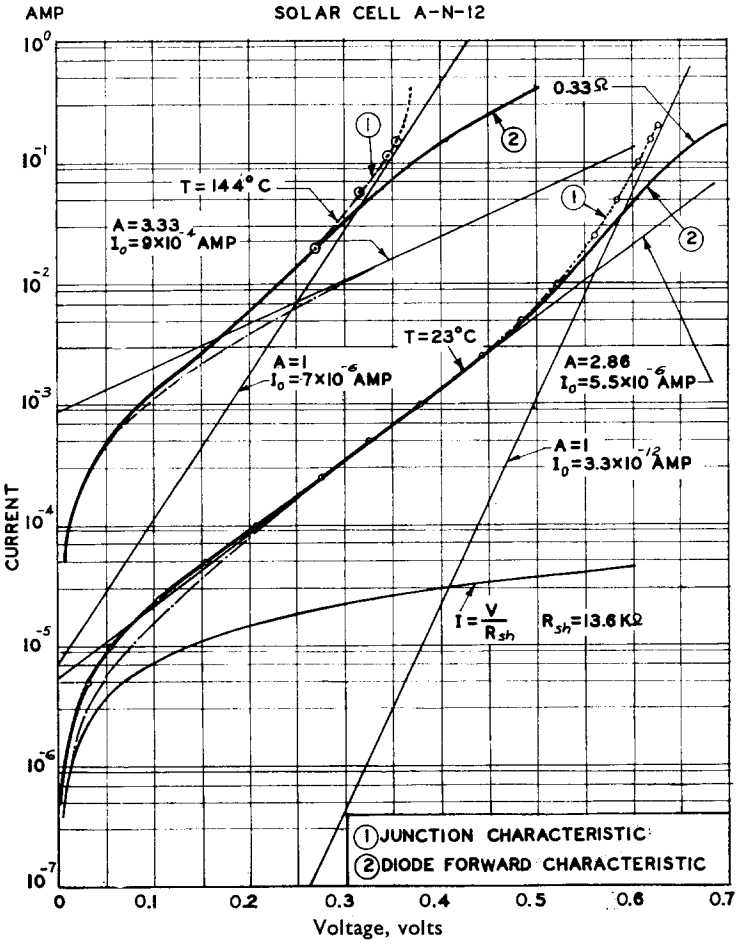


FIG. 11.

teristic, the temperature dependence of these characteristics, and for the interpretation of the physical mechanisms causing the observed device behavior. The *p–n* junction characteristic, described as method 3 in Section 2, provides a very useful supplement to the diode forward characteristic for such studies. The usefulness of the *p–n* junction characteristic stems from the severe effect which the series resistance has on the diode forward characteristic at high injection levels, and which is not present in the *p–n* junction characteristic.

At sufficiently low injection levels where series resistance effects become negligible the two characteristics become identical. Figure 11 contains a diode forward characteristic and

a *p–n* junction characteristic obtained at 23°C on the gridded solar cell A-N-12 which was used for the previously described measurements. The graph shows excellent agreement obtained between the two different methods at injection levels below $10^{-3}$ A on the 2 cm$^2$ cell. Experimentally obtained points of the *p–n* junction characteristic given by circles superimposed on the also experimentally obtained diode forward characteristic, presented by the solid curve demonstrate this agreement. Above $2 \times 10^{-3}$ A, however, divergence between the two curves is observed. The difference between the *p–n* junction characteristic and the diode forward characteristic at high injection levels corresponds to a series resistance of 0·33 $\Omega$, which differs from the 0·38 $\Omega$ value obtained from the photovoltaic output characteristic according to section 6.

Evaluation of the reverse characteristic yields a shunt resistance value of 13·8 k$\Omega$, and a saturation current $I_0 = 6{\cdot}5 \times 10^{-6}$ A. The current conducted through such a shunt resistance is shown in Fig. 11 by the curve marked "$I = V/R_{sh}$". By subtracting the current conducted through this shunt resistance from the current values of the diode forward characteristic, a new curve is obtained which deviates from the experimentally obtained characteristic at the low injection levels. The curve thus obtained is the true *p–n* junction characteristic without resistive shunt effects. The curve is matched by a diode equation of the form of equation (2) with a saturation current $I_0 = 5{\cdot}5 \times 10^{-6}$ A and constant $A = 2{\cdot}86$ at a device temperature of 296°K. At the high injection levels, however, a deviation from the exponential is observed. This deviation is in the diode forward characteristic partially hidden by the effect of the series resistance, but can be clearly observed and evaluated from the *p–n* junction characteristic.

The *p–n* junction characteristic at high injection levels asymptotically approaches a second exponential curve which in the semi-log plot of Fig. 11 is represented by a straight line. The transition region between the two pure exponential portions of the curve is very accurately described by the sum of the two exponential terms. It is interesting to note that on all solar cells thus investigated, the second exponential term has an $A$ value of 1 and saturation currents of $10^{-12}$ to $10^{-11}$ A for the 2 cm$^2$ junction. Such values are to be expected from a device following the carrier diffusion theory of a *p–n* junction as described by Shockley [9].

Also shown in Fig. 11 is a diode forward characteristic obtained on the same cell at a device temperature of 417°K. At the high injection level a series resistance voltage drop corresponding to the series resistance value of 0·33 $\Omega$ was found in the room temperature curve. This voltage drop was subtracted from the diode forward characteristic and, again, was found to lead to a good match to the *p–n* junction characteristic. The very highest current values, which were obtained by the diode forward method only, appear too high, probably due to thermal runaway during the measurements.

The resultant characteristic for the *p–n* junction at 417°K can also be best described by the super-position of two exponential terms. Like in the room temperature case, the curve approaches asymptotically the exponential represented by a straight line in the semi-log plot at the high injection levels, while the transition region is accurately described by the sum of the two exponentials.

The remarkable finding is, that the exponential for the higher injection levels has the constant $A = 1$. Using the carrier diffusion theory for *p–n* junctions as described by Shockley, and the experimental value for $I_0 = 3{\cdot}3 \times 10^{-12}$ A at 296°K, one arrives at a saturation current $I_0 = 8 \times 10^{-6}$ A for the same junction at 417°K. This is in very good agreement with the experimental finding of $7 \times 10^{-6}$ A.

While extremely good correlation between the $p$–$n$ junction characteristic at high injection levels and the carrier diffusion theory for $p$–$n$ junction behavior could repeatedly be established, no correlation to a theoretical behavior could be found for the lower injection

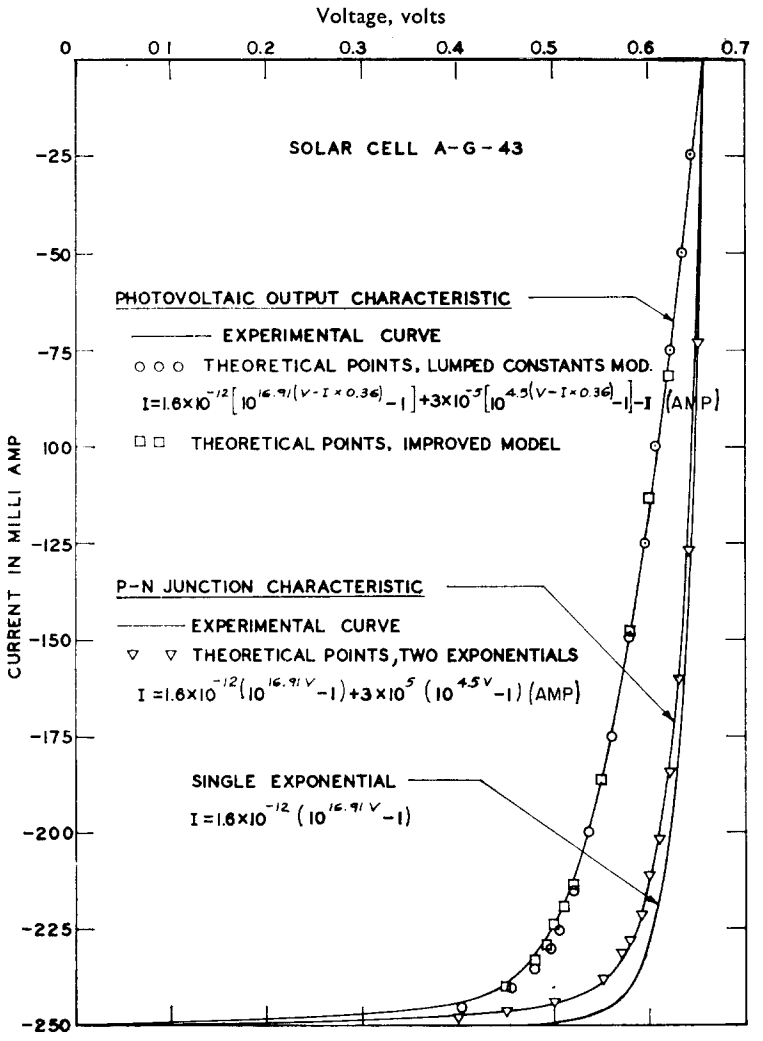


FIG. 12.

level part of the characteristic. A considerable spread of values for the constant $A$ and for the saturation current were found for the lower injection level exponential. Still more non-uniformity was observed in the temperature dependence of this portion of the curve. Since no pattern could yet be established in these findings, a hypothesis shall not be advanced for the physical nature of the characteristics at the lower current levels.

The foregoing discussions lead to a replacement of equation (1) by the following form:

$$I = I_{01}\left[\exp\left(\frac{q}{AkT}V\right) - 1\right] + I_{02}\left[\exp\left(\frac{q}{kT}V\right) - 1\right] - I_L \tag{8}$$

with $A = A(T)$, excepting the series resistance terms.

According to this description a new equivalent circuit diagram is evolved containing two separate forward biased diodes connected in parallel. This new model resembles one advanced earlier by Watson [10]. Watson, however, assigned identical exponents to both junctions, and described only a relatively small difference in the saturation currents. A separation of the two *p–n* junctions by the series resistance is not necessary, because the *p–n* junction characteristic alone exhibits the property of the super-position of the exponentials, and at high injection levels where the series resistance becomes most effective the characteristic is dominated by only one of the two exponentials.

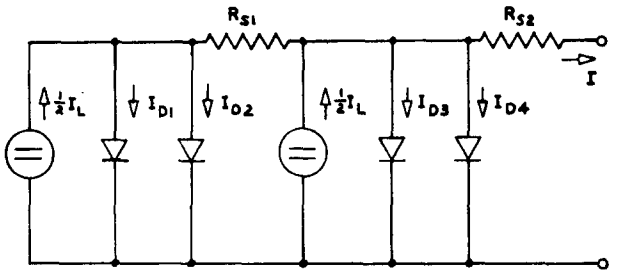


$$I_{D1} = I_{01}\left\{\text{EXP.}\left[\frac{q}{kT}\left[V - IR_{S2} - \left(I - \frac{1}{2}I_L + I_{D3} + I_{D4}\right)R_{S1}\right]\right] - 1\right\}$$

$$I_{D2} = I_{02}\left\{\text{EXP.}\left[\frac{q}{AkT}\left[V - IR_{S2} - \left(I - \frac{1}{2}I_L + I_{D3} + I_{D4}\right)R_{S1}\right]\right] - 1\right\} \qquad A = f(T)$$

$$I_{D3} = I_{01}\left\{\text{EXP.}\left[\frac{q}{kT}(V - IR_{S2})\right] - 1\right\}$$

$$I_{D4} = I_{02}\left\{\text{EXP.}\left[\frac{q}{AkT}(V - IR_{S2})\right] - 1\right\} \qquad A = f(T)$$

FIG. 13.

The knee of the *I–V* characteristic, however, is most heavily affected by the transition region between the two exponentials. This is demonstrated in Fig. 12, which shows an exponential curve with $A = 1$ and $I_0 = 1{\cdot}6 \times 10^{-12}$ A together with the experimentally obtained *p–n* junction characteristic for cell A-G-43. In the portion of the characteristic nearer the open circuit voltage point, which is the high injection region, close approximation between the two curves can be noticed. In the knee of the curve, however which falls into the transition between the two exponentials, the experimental curve appears much more rounded than the single exponential with $A = 1$. In the part of the curve approaching the short circuit current, the difference between the two exponentials is not discernible because of the scale of the plot.

The sum of two exponentials, for which the saturation currents and *A*-values have been obtained from a semi-log plot for cell A-G-43 similar to Fig. 11, has been calculated, and its results are superimposed on the experimentally obtained *p–n* junction characteristic, illustrating the good agreement.

Finally, the photovoltaic output characteristic is shown, obtained experimentally at a light intensity equivalent to about 500 mW cm$^{-2}$ of solar irradiance. Shown with this curve as circles are values calculated by using the "sum-of-two-exponentials" model together

with a single lumped series resistance corresponding to the original model of Fig. 1(a). The points obtained in this manner show a fair approximation to the experimental curve, with the largest deviations at the knee of the curve which is of greatest interest for maximum power output considerations.

A further calculation has been carried out using the improved lumped constants model described in section 7 and Fig. 10 together with the "sum-of-two-exponentials" model. The results are presented in the form of squares superimposed on the experimental curve. They prove the very close approximation to the actual cell characteristic obtained by the use of this model. The equivalent circuit diagram of this model is shown in Fig. 13, and the equation describing it has the following form:

$$I = I_{01}\left\{\exp\left[\frac{q}{kT}(V - IR_{s_2})\right] - 1\right\} + I_{02}\left\{\exp\left[\frac{q}{AkT}(V - IR_{s_2})\right] - 1\right\}$$
$$+ I_{01}\left\{\exp\left[\frac{q}{kT}[V - IR_{s_2} - (I - \tfrac{1}{2}I_L + I_{D_3} + I_{D_4})\,R_{s_1}]\right] - 1\right\}$$
$$+ I_{02}\left\{\exp\left[\frac{q}{AkT}[V - IR_{s_2} - (I - \tfrac{1}{2}I_L + I_{D_3} + I_{D_4})\,R_{s_1}]\right] - 1\right\} - I_L \qquad (9)$$

Although this model is only the next improvement step after the original lumped constants model, it exhibits already considerable complexity, but yields also much more satisfactory results.

It will be interesting to note that for cell A-G-43 the values for $R_{s_1}$ and $R_{s_2}$ which were found to give best results were 0·265 and 0·30 respectively. This compares to a single lumped resistance of $R_s = 0{\cdot}36\ \Omega$ for the old model. The values indicate a larger contribution from the sheet resistance than from the bulk and contact resistances.

The foregoing discussions shed light on the importance of the *p–n* junction characteristic to the device development engineer, who can by applying this method study the device parameters without being hindered by the overshadowing effects of series resistance.

## 9. CONCLUSION

The foregoing discussion illuminates the effect of series resistance on solar cell measurements and the caution to be taken in their interpretation. The reduction of efficiency at high light intensities due to high values of series resistance was analyzed with the conclusion that for advantageous application of solar cells at high light intensities emphasis has to be placed on the reduction of series resistance. Finally, new features of the *p–n* junction characteristic were discussed.

These were previously hidden due to the modification of the current–voltage characteristic by series resistance effects. New lumped constants models were developed which more closely approximate the characteristics measured on the solar cells.

*Acknowledgement*—Special appreciation shall be expressed to Messrs. P. Goldsmith and W. Schaefle of the Jet Propulsion Laboratory, Pasadena, California, for their mentioning of observed discrepancies between measured photo-voltaic output characteristics and the theoretical curves as described by the older lumped constants model.

## APPENDIX A

*Finding the proper* IV *characteristic for an individual solar cell or a solar cell matrix after a light level change by means to two translations of the coordinate system*

The basic equation describing the current–voltage characteristic of a solar cell neglecting series- and shunt-resistance is:

$$I = I_0 (e^{BV} - 1) - I_L \tag{A1}$$

where: $B = q/AkT$, and all other quantities as described in section 2 of the paper.

Let:

$$I_1 = I_0 (e^{BV_1} - 1) - I_{L_1} \tag{A2}$$

be equation (A1) at light level $L_1$ and

$$I_2 = I_0 (e^{BV_2} - 1) - I_{L_2} \tag{A3}$$

the same equation at light level $L_2$.

Since $V$ is the independent variable, one can choose:

$$V_2 = V_1 \tag{A4}$$

and can set:

$$I_{L_2} = I_{L_1} + \Delta I_L \tag{A5}$$

where $\Delta I_L$ is proportional to the difference in light intensity between levels 1 and 2. Subtracting equation (A2) from equation (A3) after introducing equation (A4) and (A5), one obtains:

$$I_2 = I_1 - \Delta I_L \tag{A6}$$

for all choices of $V_2 = V_1$.

Equation (A6) describes a translation of the coordinate system parallel to the current axis by the amount $\Delta I_L$ on the current axis.

For higher light levels, the effect of series resistance on the $IV$ characteristic has to be included, due to the increased magnitude of the current $I$ (see Fig. 1). Here

$$V' = V - IR_s \tag{A7}$$

is the voltage across the $p$–$n$ junction, which is larger than the terminal voltage $V$ by the voltage drop in the series resistance. (Note that the current $I$ is a negative quantity (see equation (A1)), resulting in $V' \geqslant V$ for power generation in the solar cell (4th quadrant operation). The $IV$ characteristic for the equivalent circuit (Fig. 1(a)) is:

$$I = I_0 (e^{B(V - IR_s)} - 1) - I_L \tag{A8}$$

$$= I_1 (e^{BV'} - 1) - I_L \tag{A8a}$$

Introducing again two light levels 1 and 2, one obtains:

$$I_1 = I_1 (e^{BV'_1} - 1) - I_{L_1} \tag{A9}$$

$$I_2 = I_1 (e^{BV'_2} - 1) - I_{L_1} - \Delta I_L \tag{A10}$$

Again one chooses:

$$V'_2 = V'_1 \tag{A11}$$

and obtains the same translation as before:

$$I_2 = I_1 - \Delta I_L \tag{A6}$$

Equation (A7) results, however, in two different terminal voltages $V_1$ and $V_2$ for the two currents $I_2$ and $I_1$. From equations (A11), (A7) and (A6), follows:

$$V_1 - I_1R_s = V_2 - I_1R_s + \Delta I_L R_s \tag{A11a}$$

which describes a constant relationship between $V_1$ and $V_2$ for any choice of $V_1$. The constant of this relationship is proportional to the series resistance $R_s$ and to the change in light level. Equation (A11a) thus describes a second translation of the coordinate system, this one parallel to the voltage axis by the amount:

$$V_2 = V_1 - \Delta I_L R_s \tag{A12}$$

Equations (A6) and (A7) describe the photovoltaic output characteristic as invariant to any change in the light intensity except for two translations of the (current–voltage) coordinate system.

## REFERENCES

[1] H. RAUSCHENBACH, Understanding Solar Measurements, *Semicond. Prod. Applic. News.* Hoffman Electronics Corp., El Monte, Calif. (1960).
[2] W. G. PFANN and W. VAN ROOSBROECK, *J. Appl. Phys.* **25**, 1422 (1954).
[3] M. B. PRINCE, *J. Appl. Phys.* **26**, 534–540 (1955).
[4] M. WOLF and M. B. PRINCE, "New Developments in Silicon Photovoltaic Devices and Their Application in Electronics", plublished in *Solid State Phys. Electron. Telecom.*, Proc. Int. Conf. Brussels, Belgium, June 2–7, 1958, **2**, 1180–1196, Academic Press, New York (1960).
[5] A. J. HEEGER and T. R. NISBET, The Solar Cell Diode Curve, Rept. LMSD No. 310003, Lockheed Missile Systems Division, Sunnyvale, California (1958).
[6] H. J. QUEISSER, *Solid State Electron.* **5**, 1 (1962).
[7] L. D. SWANSON, private communication.
[8] J. J. WYSOCKI, J. J. LOFERSKI and P. RAPPAPORT, *Research on Photovoltaic Converters*, Proc. 14th Ann. Power Sources Conf., pp. 32–36, Power Sources Div., U.S. Army Signal Res. and Dev. Lab., Ft. Monmouth, N.J. (1960).
[9] W. SHOCKLEY, *Electrons and Holes in Semiconductors*, Van Nostrand, New York (1950).
[10] R. H. WATSON, *Equivalent-circuit Characteristics of the Solar Cell.* Presented at the 1960 Pacific General Meeting of the AIEE at San Diego, California, August 11, 1960.

**Zusammenfassung**—Strom–Spannungs-Charakteristiken von photoelektrischen Sonnen-energie-Umwandlern kann man nach drei verschiedenen Methoden erhalten. Durch den Einfluss des Innenwiderstandes der Zellen liefert jede ein anderes Ergebnis. Die drei resultierenden Charakteristiken sind: (1) Die photoelektrische Ausgangs-Charakteristik, (2) die *p–n*-Übergang-Charakteristik und (3) die Gleichrichter-Durchlass-Charakteristik. Um die für die individuelle Anwendung richtige Information zu erhalten, muss in jedem Fall die geeignete Methode ausgewählt werden.

In den meisten Fällen wird die photoelektrische Ausgangs-Charakteristic benutzt, z.B. für die Bestimmung der Leistung von Sonnenenergie-Umwandlern. Es wird eine Methode beschrieben, die es gestattet, eine solche Charakteristick für eine beliebige Lichtintensität aus einer entsprechenden anderen mit davon verschiedener Lichtintensität rasch herzuleiten. Die Methode benutzt zwei Koordinaten-Transformationen und erfordert nur die Kenntnis des Innenwiderstandes und die Abhängigkeit der Kurzschluss-Ströme von der Intensität.

Eine Umkehrung dieser Methode erlaubt eine einfache Bestimmung des Innenwiderstandes. Dazu genügen Messungen bei zwei beliebigen Intensitäten unbekannter Grösse.

Die Wirkung des Innenwiderstandes bei hohen Lichtintensitäten besteht in einer Abflachung der photoelektrischen Ausgangs-Charakteristic und damit einem Abfall der Spannung bei der grössten Leistung. Die daraus resultierende Verkleinerung des Wirkungsgrades muss bei Anwendung von optischen Konzentratoren oder bei Verwendung im Weltraum in grösserer Sonnennähe durch Erniedrigung des Innenwiderstandes ausgeglichen werden. In Zellenbereichen grösseren Abstands vom Kontaktstreifen wächst die Spannung an und erreicht bei grossen Intensitäten fast die Verhältnisse beim offenen Stromkreis. Das bedingt eine Stromverdrängung von diesen Bereichen der Zelle und eine Abweichung von der normalen Proportionalität von Kurzschluss-Stom und Lichtintensität.

Die direkte Messbarkeit der *p–n*-Übergang-Charakteristik nach der zweiten Methode ohne Innenwider-

standseffekte bei hohen Stromdichten erweist sich als hervorragendes Werkzeug für den Entwicklungsingenieur und liefert daneben noch eine zweite Möglichkeit für die Bestimmung des Innenwiderstandes.

Die Ergebnisse der Anwendung dieser Methode zeigen, dass die Charakteristik der Silizium-Photozelle im Stromdichte-Bereich der Sonnenbatterien durch die Diffusionstheorie für *p–n*-Übergänge weit besser beschrieben wird, als man früher angenommen hatte.

**Résumé**—Les caractéristiques Intensité–Tension des cellules de convertisseurs d'énergie solaire photovoltaïques peuvant être obtenues par trois méthodes qui donnent des résultats différents par suite des effets de résistance intérieure en série des cellules. Les trois caractéristiques résultantes sont: (1) la caractéristique de rendement photovoltaïque, (2) la caractéristique de jonction *p–n*, et (3) la caractéristique de redresseur (vers l'avant). Pour obtenir le renseignement correct relatif à l'application particulière, il est nécessaire de choisir la méthode appropriée.

La caractéristique de rendement photovoltaïque est utilisée très fréquemment, par exemple, pour la détermination de la performance du convertisseur solaire. Il est décrit un procédé rapide permettant de tirer cette caractéristique pour tout niveau de lumière d'une caractéristique correspondante obtenue pour un niveau de lumière différent. Cette méthode fait intervenir deux translations du système de coordonnées et n'exige que la connaissance de la résistance en série et de la différence des intensités lumineuses des courants de court-circuits.

Une inversion de cette méthode permet de déterminer facilement la résistance en série, en faisant intervenir des mesures à deux niveaux de lumières arbitraires de grandeur non connue.

A des niveaux lumineux élevés les effets de la résistance en série se traduisent par un aplatissement de la caractéristique de rendement photovoltaïque et en une chute de la tension du point de puissance maximum. La diminution de rendement résultante doit être neutralisée par réduction des résistances en série pour des applications de cellules solaires avec moyens de concentration optiques, ou bien pour des missions spatiales à proximité du soleil. Dans les parties des cellules, progressivement plus éloignées de la bande de contact, il se produit des tensions de cellules croissantes se rapprochant de l'état de circuit ouvert à des intensités lumineuses très élevées, ce qui donne lieu à une réduction de l'apport de courant provenant de ces parties de cellules et à une déviation de la proportionalité normale entre le courant de court-circuit et l'intensité lumineuse. La mesurabilité directe par la deuxième méthode de la caractéristique de jonction *p–n* à des densités de courant élevées sans effets de résistance en série met à la disposition de l'ingénieur de mise au point un instrument puissant et, en outre, procure une deuxième méthode de détermination de la résistance en série. Les résultats de l'application de cette méthode indiquent que dans la gamme des densités de courants utilisées dans la conversion de l'énergie solaire, la caractéristique des cellules solaires au silicium est décrite par la théorie de la diffusion pour des jonctions *n–p* avec beaucoup plus de précision qu'on ne l'avait pensé auparavant.